

Influence of the Mesh Size on the Computation of the Close Near Fields of Dipole Antennas

ALESSANDRA PAFFI¹, EDUARDO CARRASCO² (Senior Member, IEEE),
AND QUIRINO BALZANO³ (Life Fellow, IEEE)

¹Department of Information Engineering, Electronics and Telecommunications, Sapienza University of Rome, 00184 Rome, Italy

²Information Processing and Telecommunications Center, Universidad Politécnica de Madrid, 28040 Madrid, Spain

³Department of Electrical and Computer Engineering, University of Maryland at College Park, College Park, MD 20742, USA

CORRESPONDING AUTHOR: A. PAFFI (e-mail: alessandra.paffi@uniroma1.it).

ABSTRACT While evaluating the near field of dipole antennas, it is noted that different software suites yield values of the electric and the magnetic fields, at the surface of antennas, that can be substantially different, especially at the tips and at the feed gap. The close near field of dipoles has not been yet analysed in detail. An asymptotic expansion method for the near fields at the surface of these antennas has been developed and compared to the computed fields. The results show that the software of the computed field should not use a uniform mesh. The mesh should be much tighter at the metal extremities than in the dipole body. The proposed technique can be used to check complex field computations, producing diverging values, with simple analytical equations.

INDEX TERMS Dipole antennas, near fields, computational electromagnetics, asymptotic expansion.

I. INTRODUCTION

THE CLOSE near field ($< \lambda/2\pi$) of dipoles has not been the object of detailed analysis because, for wireless technologies, antennas are spaced at much greater distances. Relatively few authors [1], [2], [3], [4], [5], [6], [7], [8] have investigated the close near field of thin and thick dipoles, mainly using integral equation solutions.

Recently, there has been a proliferation of radiating devices whose antennas can be very close to each other or to electronic circuits of vital importance in human health. The analysis of interference phenomena can require the evaluation of magnetic (H) and electric (E) fields extremely close to their sources.

The advent of finite element analysis enabled the evaluation of the near field of dipoles without using integral equation analysis. However, as shown below, if the computational mesh is not carefully selected, the resulting near fields are asymmetric with respect to the feed point of the antenna. The computational approach presented in this paper is a merger, a hybrid, of the finite element method analysis and the asymptotic expansion of the cylindrical functions that express the field amplitude dependence on the radial

distance from the surface of the dipole. It simplifies evaluation of E and H fields at arbitrarily close distances from the surface of dipoles, because it does not require the computation of the field contributions of the various current elements at one observation point very close to the antenna surface.

The current on a cylindrical dipole, its first and second derivatives are continuous functions of the axial coordinate except at the tips and at the feeding gap of the antenna, where diverging, high intensity, displacement currents originate or terminate, while the electric current always remains finite [9]. To compute the fields on the surface of a perfectly conducting dipole or arbitrarily close to it, it may be convenient to evaluate the current function and its derivatives without having to resort to exceedingly tight finite difference mesh that can cause computational instabilities in the field numerical values. This is possible by using asymptotic expansions of E and H fields that are valid close to the antenna surface.

In this paper, to compute the very close near fields of dipoles, we have used two widely available suites: Comsol Multiphysics[®], RF module, and the Frequency Domain

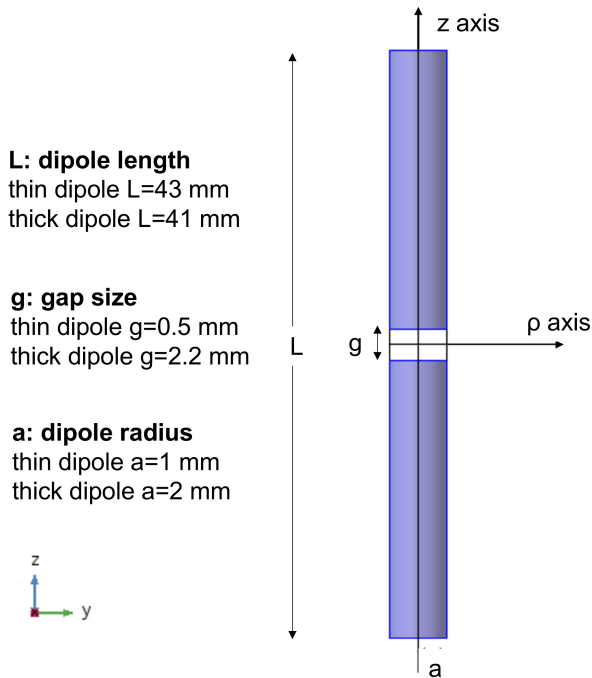


FIGURE 1. Dipole geometry and coordinate system.

Solver of CST Studio [®], which are based on the finite element method (FEM). Both approaches have numerical incongruences as the computational field domain approaches the surface of the dipoles as shown later in the text. The FEM computed results are compared with the field values derived by using very simple asymptotic equations.

This paper presents the advantages of using a dual approach (theory of functions and finite element software tools) to the evaluation of E and H fields very close to their sources where these fields can have large values that are difficult to evaluate accurately with only finite element digital analytical tools. This is a novel approach to the analysis of electromagnetic fields very close to their sources.

II. ANALYTICAL APPROACH

We have considered a “thin” (1 mm radius) and a “thick” (2 mm radius) resonant dipole to evaluate the H field, the axial and radial components of the E field using both the values computed by the suites and the asymptotic expansions.

Using the CST software for the computation of the antenna impedance, the thin dipole resonant length at 3 GHz ($R = 71 \Omega$, $X = 0. \Omega$) is 45 mm with 0.5 mm feeding gap. The thick dipole resonant ($R = 69 \Omega$, $X = 0. \Omega$) length is 41 mm with 2.2 mm feeding gap.

With the Comsol Multiphysics software at 3 GHz and the same antenna dimensions, the thin dipole has a driving impedance of $R = 76 \Omega$, $X = 0.1 \Omega$. The thick dipole at 3 GHz has a driving point impedance of $R = 69 \Omega$, $X = -j9.2 \Omega$.

Fig. 1 shows the geometrical dimensions of the resonant dipoles.

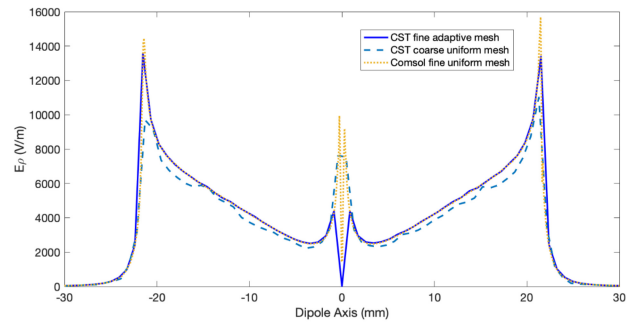


FIGURE 2. Mesh density effect on the radial E-field component.

The results for the current density, the H field and the two E-field components E_ρ (radial) and E_z (axial) will be presented in Section III-A, III-B, and III-C, respectively, with the corresponding values from the asymptotic expansion. A summary and some concluding remarks are given in the final section. The asymptotic equations for the fields are given in the Appendix.

III. FIELDS COMPUTATION

A good example of the uncertainty of the results of the fields near a dipole is shown in Fig. 2, which plots the radial E field for the thin dipole at $\rho = 1.1$ mm.

As expected, the computed field values are different for the coarse and the fine computational meshes. However, even the field evaluated with fine uniform meshes presents different peak and gap values. In the following, the proposed asymptotic analytical method is presented in detail for all field components.

A. MAGNETIC FIELD

Fig. 3 plots the H field for 1 W input power to the thin (panels a and b) and the thick (panels b and c) dipole, using either Comsol (panels a and c) or CST (panels b and d) computational suites. The H field was calculated along 6 lines parallel to the dipole axis at different distances from the antenna surface and has the same value over the length of the dipole as the axial current density. In Fig. 3, the axial current density shows clearly a discontinuity at the feed gap and at the tips of the antenna. With 1 W excitation and $R = 71 \Omega$, the current at the feed point is $I = 1/\sqrt{71} = 0.118$ A. The current density near the feed point is simply $J = 0.118/(2\pi \cdot 0.001) \text{ A/m} = 18.88 \text{ A/m}$, which is also the value of the H field. In Fig. 3, as expected, the asymptotic expansion of the H field does not provide values past the tips of the antenna for any radial distance while computed results show that the H field decays rapidly past the ends of the dipole.

For the H field near the thicker dipole, the peak value of the current density and of the H field are approximately half of those of the thin dipole because of the doubling of the antenna radius.

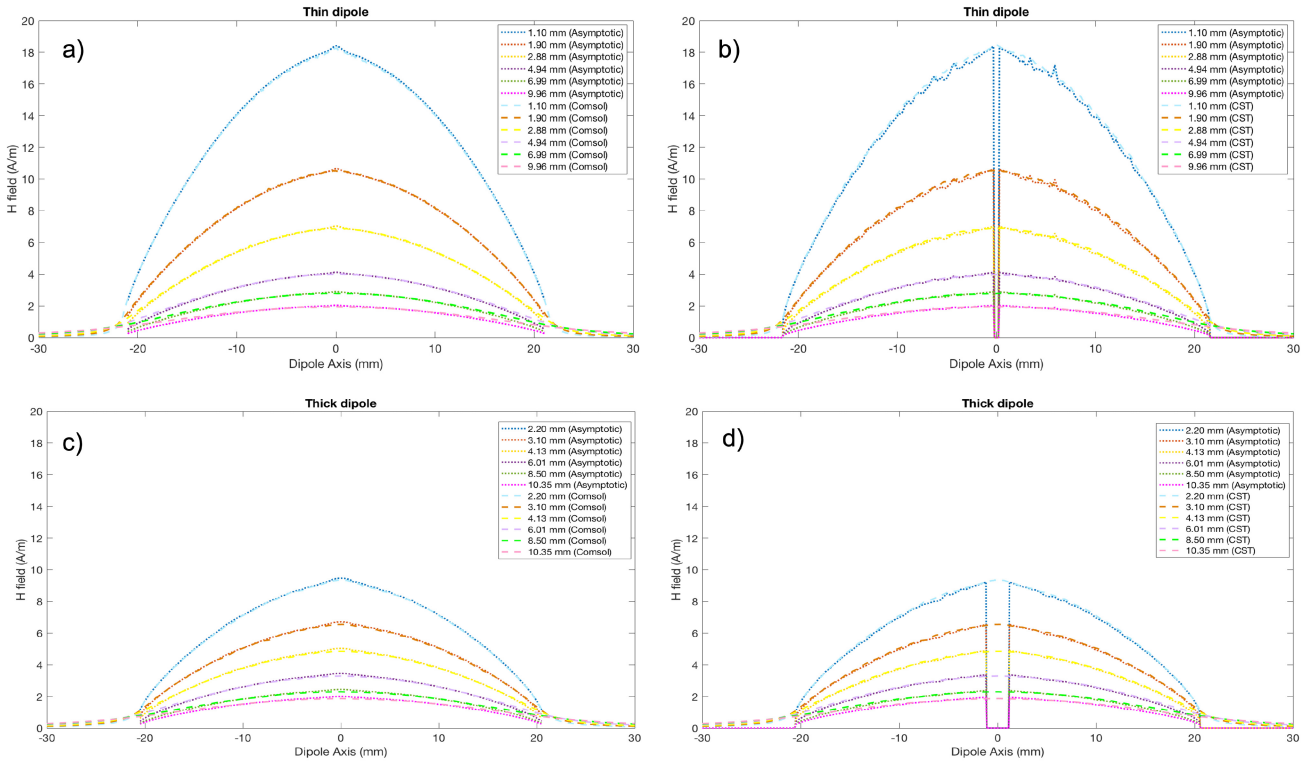


FIGURE 3. H field near the dipole.

The results of Fig. 3 show that the H-field pattern on the surface of the dipole can be computed using the simple equation A3 given in the Appendix.

B. RADIAL ELECTRIC FIELD

The radial E field (REF) diverges at the metal tips and at the edge of the feeding gap of the dipole because its sources are the electric charges on the surface of the antenna created by the discontinuity of the antenna current density. The discontinuities of the current density at the metal edges are step functions, so the charge density at such locations is infinite. The diverging amplitude of the local E fields is bound by the amount of the stored electric energy at the current discontinuities [10]. See Fig. 4 which shows half a dipole and the location of one of the field singularities.

In the planar edge [10] in the domain with radius R the stored electric energy is finite by the requirement that the modulus of the E field is bound by the following relation:

$$\int_0^R |E(\rho)|^2 \rho d\rho < \infty \quad (1)$$

Then $|E(\rho)|$ must have the functional form: $\rho^{-1+\alpha}$ for $\rho \rightarrow 0$ with $\alpha > 0$.

In the case of a cylindrical edge, because of rotational symmetry, the E fields have identical distribution in the toroidal volume whose cross section is shown in Fig. 4.

Equation (1) gives the electric energy stored at a cross section of a straight edge. Because of rotational symmetry,

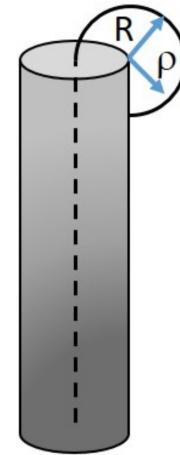


FIGURE 4. Cylindrical edge singularity.

the total electric energy at a tip of a cylindrical dipole is given by:

$$\int_0^{2\pi} \left[\int_0^R |E(\rho)|^2 \rho \right] \rho d\phi d\rho < \infty \quad (2)$$

This last integral shows that $|E(\rho)|$ has the functional form: ρ^{-1} .

To check the edge approximations provided by the two widely used suites mentioned above, the following E-field computations were performed with 1 W power applied to the feeding gap of the dipole. Since the charge density is the

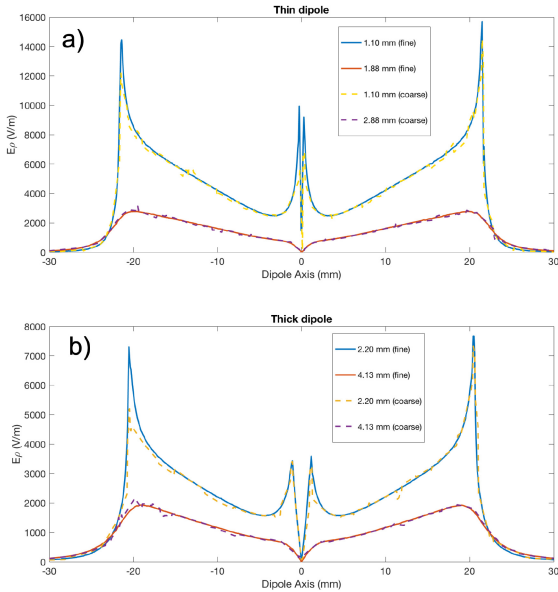


FIGURE 5. Radial E field for the thin (panel a) and thick (panel b) dipoles using fine and coarse meshes.

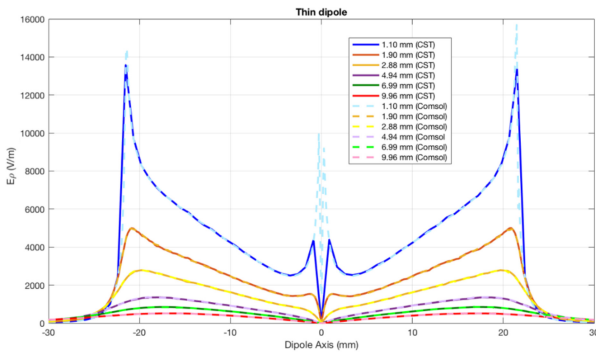


FIGURE 6. Radial E field. CST and Comsol results for the thin dipole.

derivative of the current density, the amplitude of the radial E field (REF) depends on how fine is the mesh selected for the computations. Fig. 5b shows the REF results for the thick dipole using a very fine Comsol mesh ($d = 0.5$ mm) and a more relaxed mesh ($d = 3$ mm) at 2.2 mm and 4.13 mm distances from the axis of the dipole (0.002λ and 0.0038λ from the antenna surface). For the shortest distance, the field pattern calculated with the coarse mesh loses the symmetry and underestimates the field value in correspondence of the current discontinuity at one end of the dipole. For greater distances, the field patterns calculated using the coarse and the fine meshes become much more similar, except for higher fluctuations obtained with the coarse mesh, as expected.

Similar results are found for the thin dipole as shown in Fig. 5a, with discrepancies observed along the closest line to the dipole in correspondence of the points with current discontinuities.

Fig. 6 shows the radial near field for the thin dipole evaluated using Comsol with a very fine mesh (0.5 mm) and using the CST with a mesh with an inhomogeneous adaptive

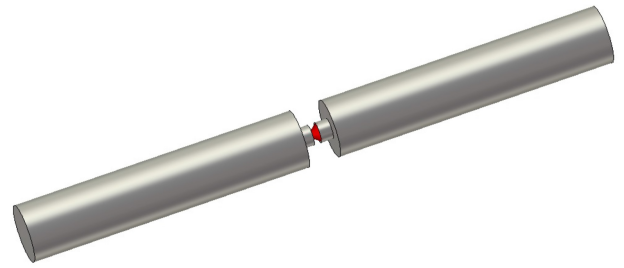


FIGURE 7. Thick dipole gap modification.

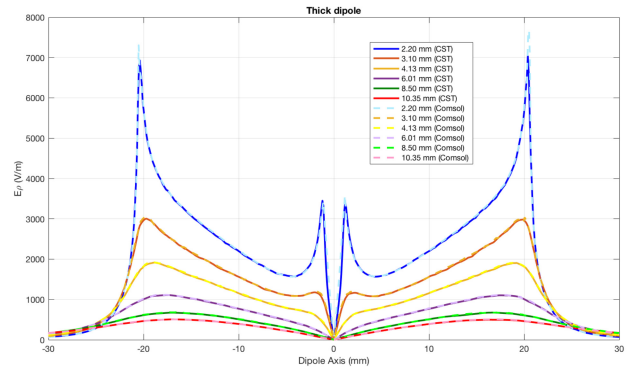


FIGURE 8. Radial E field. CST and Comsol results for the thick dipole.

tetrahedral mesh refinement. Looking at the closest distance (1.10 mm), the field patterns are similar but the peak values at the current density discontinuities are very different, probably due to the different mesh refinements used by the two calculation suites.

Fig. 6 shows that, at the radial distance of 1.90 mm ($\lambda/15\pi$), the REF patterns computed with either suite yield practically similar results for the thin dipole; the similarity is stronger for greater radial distances.

The computed values also depend on mesh step size and how closely the mesh abuts the discontinuity of the axial current density. The REF amplitudes at and in the feeding gap originate from a discontinuity of the current density, so their values depend on how the computational mesh approaches the boundary of the gap. Near the surface of the antenna, different mesh size and geometry can yield different REF values at the current discontinuity.

In the case of the thicker dipole, the CST computational suite yielded inappropriate results for the REF when the gap is 2.2 mm. In order to improve the results, it was possible to modify the computational geometry of the antenna by inserting a cylindrical step in the center of the gap as shown in Fig. 7. The radius of the inserted cylinder is 0.7 mm, with a length for the port of 0.5 mm (represented with a red arrow in Fig. 7). The modified structure yielded the results in Fig. 8, which are in agreement with those of Comsol.

As shown in the Appendix, the radial component of the field has the following relation with the antenna current:

$$E_{\rho}(\rho, z) = \frac{j\eta}{2\pi k\rho} \frac{dI(z)}{dz} \quad (3)$$

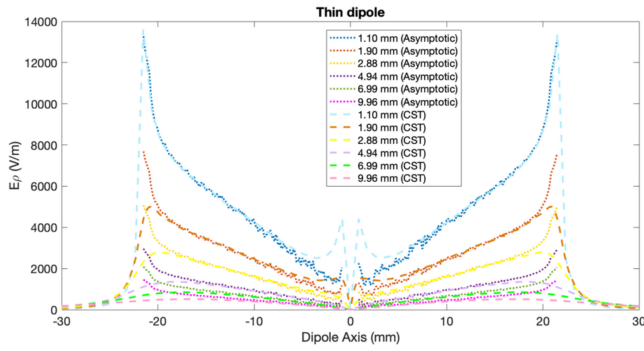


FIGURE 9. Asymptotic plot of the thin dipole radial E-field component.

The fields at a distance $\rho \geq a$ could be evaluated by a simple multiplication factor if the axial current density and its derivative have been computed.

Fig. 9 compares the values from equation (3) and those from computations with the CST software for the thin dipole. Fig. 9 shows that the REF is given by the derivative of the surface current density on the antenna. The asymptotic expansion peak values depend on the evaluation of the current density on the dipole near the metal discontinuity. For the closest distance, the plot shows a very good agreement of computed and asymptotic values except near the feed gap of the dipole. The asymptotic equation yields sharp peaks in correspondence of the tips at radial distances larger than 0.03λ from the antenna; the peaks are absent from the computational results. The disagreement is due to the contribution to the field amplitudes from charges further away from the tip of the dipole, as the radial distance from the antenna increases, but it clearly shows that the asymptotic formula gives correct results for the closest distance from the thin dipole.

C. AXIAL ELECTRIC FIELD

The tangential component of the E field should diverge at the edge of the gap because of the presence of a cylindrical metal wedge [10] as discussed in Section III-B for the radial component.

As shown in the Appendix, the axial component of the E field can be expressed by:

$$E_z(\rho, z) = \frac{-\eta}{8\pi k} \int_{-\infty}^{\infty} H_0\left(\rho\sqrt{k^2 - \zeta^2}\right) \left[\int_{-h}^h I(z') e^{jz'\zeta} dz' \right] \times (k^2 - \zeta^2) e^{-jz\zeta} d\zeta \quad (4)$$

This relation does not lend itself to a simple asymptotic evaluation because the local values of the field on the surface of the source depend from the current (and its second derivative) over the entire dipole as shown by the H_0 Hankel function which involves an integral (around two branch points) of all the infinite number of cylindrical wavelets emanating from the current everywhere on the surface of the dipole. Some additional considerations about the asymptotic behavior of

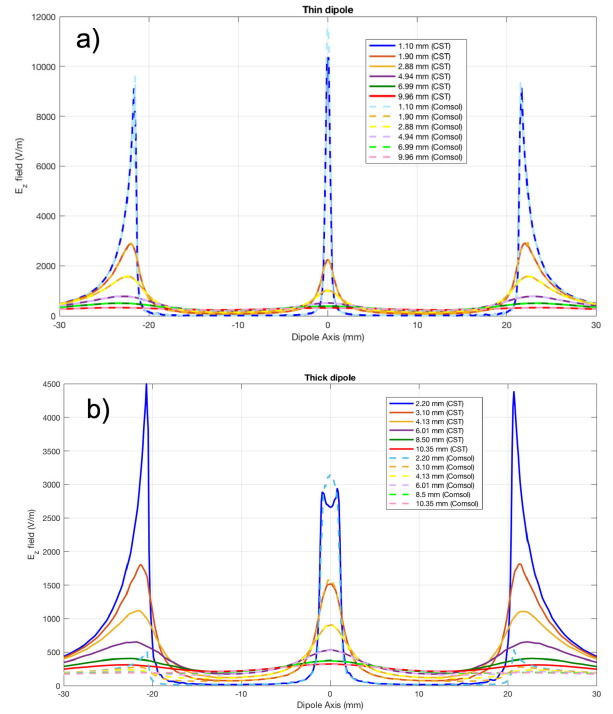


FIGURE 10. Axial E field. CST and Comsol results for the thin (panel a) and thick (panel b) dipoles.

E_z for $\rho \rightarrow a$ are given in Appendix-C, where the following relation is established:

$$E_z(\rho, z) = \frac{1}{2\pi} \left[\frac{1}{j\omega\epsilon_0} \frac{d^2}{dz^2} I(z) - j\omega\mu_0 I(z) \right] \ln\left(\frac{\rho}{a}\right) \quad (5)$$

Figs. 10a and 10b show the tangential component of the E field (TCE) at various distances from the axes of the two dipoles, computed with the Comsol and the CST suites.

Figs. 10a and 10b show very good agreement between computed results, except at the current discontinuity, especially at the ends of the thick dipole. As expected, the tangential E field tends to very low values independently from the z coordinate over the metal surface of the antenna as $\rho \rightarrow a$. An exploded view of E_z in the interval $0.011\lambda < \rho < 0.017\lambda$ is shown in Figs. 11a and 11b for the thin and the thick dipole.

The plots show a progressive flattening of the field near a minimum value at the various distances. However, the asymptotic equation does not yield the functional radial change of computed values of the TEF. Equation (4) presents a field profile of $E_z = 0$ V/m over the metal of the antenna and diverging values at the tips and the feed gap of the dipole. The computed values show this trend. The logarithmic behavior of the TEF as the observation point moves arbitrarily close to the surface of the antenna can be seen in the graphics of Fig. 11a for the thin dipole. The computations for the thick dipole show an analogous trend (Fig. 11b).

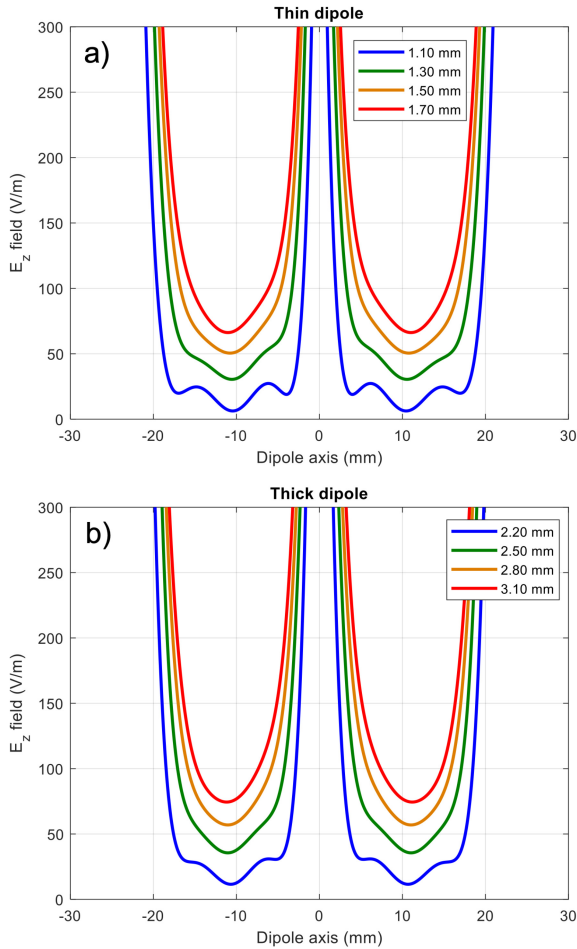


FIGURE 11. Very close axial E field for the thin (panel a) and the thick (panel b) dipoles.

IV. CONCLUSION

Both computational suites yield very similar E and H field results for radial distances from the axis of the antenna greater than $\lambda/(20\pi)$.

The asymptotic expansions proposed in this paper have a limited capacity of handling the discontinuity of the current density at the feed point of the antenna. While it is possible to use the asymptotic expansion of the H field because the current density is a continuous function over the metal of the antenna with only finite discontinuities at the feed gap and at the tips of dipole. At these locations, the derivative of the current density diverges and it makes difficult to evaluate the E fields at these points. The asymptotic expansion yields results analogous to those using very fine meshes (see Fig. 9a) at very close distance from the tip of the antenna where the radial E field has its maximum value. For this reason, it is important that the computational mesh be very dense at the feed gap and at the antenna tips for the computations of fields at distances extremely close ($< \lambda/20$) to the surface of the dipole. At these locations, the E fields have diverging amplitude.

This paper has examined also the effect of feeding gap dimension on the E-field values. The gap causes the

divergence of the local radial and axial E-field components. In the immediate vicinity of the gap there are some electric spillover charges that support the radial E field on the metal at and near the gap edges. This part of the radial field can be evaluated if the computed current density and/or H field have a finite discontinuities of the derivative near the gap. This paper also shows that the tangential E field has a logarithmic asymptotic behavior as the observation point approaches the antenna surface.

In summary, in those applications requiring the calculation of the E and H fields extremely close to the dipole (radial distance $< \lambda/20$), an adaptive non uniform mesh along the dipole's length represents the best compromise between computational time and accuracy of the estimated fields, particularly in correspondence of the antenna's edges.

The H field and the maximum value of the REF can be also conveniently estimated in the close proximity of the antenna using the asymptotic expansion proposed here.

APPENDIX ASYMPTOTIC EXPANSION OF THE FIELDS NEAR DIPOLE ANTENNAS

A. VECTOR POTENTIAL AND RADIAL ELECTRIC FIELD

With $k = 2\pi/\lambda$ the vector potential from the currents on a dipole antenna of radius “a” and length 2h is [11]:

$$A(\rho, z) = \frac{1}{8\pi j} \int_{-\infty}^{\infty} J_0(a\sqrt{k^2 - \zeta^2}) H_0^{(2)}(\rho\sqrt{k^2 - \zeta^2}) \times \left[\int_{-h}^h I(z') e^{jz'\zeta} dz' \right] e^{-jz\zeta} d\zeta \quad (A1)$$

From (A1) and [12]

$$E_\rho(\rho, z) = \frac{1}{j\omega\epsilon_0} \frac{\partial^2}{\partial\rho\partial z} A_z(\rho, z)$$

$$E_\rho(\rho, z) = \frac{-j\eta}{8\pi k} \int_{-\infty}^{\infty} \zeta J_0(a\sqrt{k^2 - \zeta^2}) H_1^{(2)}(\rho\sqrt{k^2 - \zeta^2}) \times \sqrt{k^2 - \zeta^2} \left[\int_{-h}^h I(z') e^{jz'\zeta} dz' \right] e^{-jz\zeta} d\zeta$$

In [13] it is shown that for $2\pi a/\lambda \ll 1$ $J_0(a\sqrt{k^2 - \zeta^2}) \approx 1$ and [15] that for $2\pi\rho/\lambda \ll 1$, $H_1^{(2)}(\rho\sqrt{k^2 - \zeta^2}) \approx \frac{-j2}{\pi\rho\sqrt{k^2 - \zeta^2}}$.

The asymptotic equation for the radial component of the E field $E_\rho(\rho, z)$ is expressed by:

$$E_\rho(\rho, z) = \frac{-\eta}{4\pi^2 k \rho} \int_{-\infty}^{\infty} \zeta \left[\int_{-h}^h I(z') e^{jz'\zeta} dz' \right] e^{-jz\zeta} d\zeta$$

$$= \frac{j\eta}{4\pi^2 k \rho} \int_{-\infty}^{\infty} (-j\zeta) \left[\int_{-h}^h I(z') e^{jz'\zeta} dz' \right] e^{-jz\zeta} d\zeta$$

$$= \frac{j\eta}{2\pi k \rho} \frac{dI(z)}{dz} \quad (A2)$$

The equation (A2) shows that very close to and on the surface of the antenna ($\rho = a \ll \lambda$) the radial field decays approximately as $1/\rho$. The relation is valid for distances from the antenna surface where the values of E_ρ are defined by the nearest charge density.

B. MAGNETIC FIELD

$$\begin{aligned}
 H_\theta(\rho, z) &= \frac{-1}{8\pi j} \frac{\partial}{\partial \rho} \int_{-\infty}^{\infty} J_0\left(a\sqrt{k^2 - \zeta^2}\right) H_0^{(2)}\left(\rho\sqrt{k^2 - \zeta^2}\right) \\
 &\quad \times \left[\int_{-h}^h I(\zeta') e^{j\zeta'\zeta} dz' \right] e^{-jz\zeta} d\zeta \\
 &= \frac{1}{8\pi j} \int_{-\infty}^{\infty} J_0\left(a\sqrt{k^2 - \zeta^2}\right) H_1^{(2)}\left(\rho\sqrt{k^2 - \zeta^2}\right) \\
 &\quad \times \sqrt{k^2 - \zeta^2} \left[\int_{-h}^h I(\zeta') e^{j\zeta'\zeta} dz' \right] e^{-jz\zeta} d\zeta
 \end{aligned}$$

As for the radial E field, with $2\pi a/\lambda \ll 1$

$$J_0\left(a\sqrt{k^2 - \zeta^2}\right) \approx 1 \text{ and}$$

$$H_1^{(2)}\left(\rho\sqrt{k^2 - \zeta^2}\right) \approx \frac{-j2}{\pi\rho\sqrt{k^2 - \zeta^2}} \text{ for } 2\pi\rho/\lambda \ll 1;$$

the H field is given by:

$$H_\theta(\rho, z) = \frac{-1}{4\pi^2\rho} \int_{-\infty}^{\infty} \left[\int_{-h}^h I(\zeta') e^{j\zeta'\zeta} dz' \right] e^{-jz\zeta} d\zeta = \frac{-1}{2\pi\rho} I(z) \quad (\text{A3})$$

This is the magnetostatics law of Biot-Savart. Eq. (A3) is correct very close to the antenna ($\rho \approx a$) and it is valid for larger distances ($a < \rho \leq \lambda/2\pi$) because no derivative of the current is involved in the computation of the H field.

C. AXIAL ELECTRIC FIELD

From Eq. (A1) and [12]:

$$\begin{aligned}
 E_z(\rho, z) &= \frac{1}{j\omega\epsilon_0} \left(k^2 - \frac{\partial^2}{\partial z^2} \right) A_z(\rho, z) \\
 &= \frac{-\eta}{8\pi k} \int_{-\infty}^{\infty} J_0\left(a\sqrt{k^2 - \zeta^2}\right) H_0\left(\rho\sqrt{k^2 - \zeta^2}\right) \\
 &\quad \times \left[\int_{-h}^h I(\zeta') e^{j\zeta'\zeta} dz' \right] \left(k^2 - \zeta^2 \right) e^{-jz\zeta} d\zeta
 \end{aligned}$$

The J_0 Bessel function is given by the following series [13]:

$$J_0\left(a\sqrt{k^2 - \zeta^2}\right) = 1 - \frac{a^2}{4} \left(k^2 - \zeta^2 \right) + \frac{a^4}{16} \left(k^2 - \zeta^2 \right)^2 - \dots$$

With $ak/2 \ll 1$, the function J_0 can be approximated by the first term of the above series as in the previous asymptotic formulations.

$$\begin{aligned}
 E_z(\rho, z) &= \frac{1}{j\omega\epsilon_0} \left(k^2 - \frac{\partial^2}{\partial z^2} \right) A_z(\rho, z) \\
 &= \frac{-\eta}{8\pi k} \int_{-\infty}^{\infty} H_0\left(\rho\sqrt{k^2 - \zeta^2}\right) \left[\int_{-h}^h I(\zeta') e^{j\zeta'\zeta} dz' \right] \\
 &\quad \times \left(k^2 - \zeta^2 \right) e^{-jz\zeta} d\zeta \quad (\text{A4})
 \end{aligned}$$

This relation does not lend itself to a simple asymptotic evaluation because the local values of the field on the surface of the source depend from the current (and its second derivative) over the entire dipole as shown by the H_0 Hankel function which involves the integral (around two branch points) of

all the infinite number of cylindrical wavelets emanating from the current everywhere on the surface of the dipole. For extremely thin dipoles $2\pi a/\lambda \rightarrow 0$, the tangential E field E_z is a logarithmic function of the radial coordinate as shown below.

From the asymptotic functions of the H field and the radial component of the E field,

$$\begin{aligned}
 \vec{H}_\theta(\rho, z) &= \frac{-1}{2\pi\rho} I(z) \vec{\theta}_o, \\
 \vec{E}_\rho(\rho, z) &= \frac{1}{j\omega\epsilon_0} \frac{\partial I(z)}{\partial z} \vec{\rho}_o
 \end{aligned}$$

and the rotation of the E field we find the following relation for E_z :

$$\begin{aligned}
 \nabla \times \vec{E} &= -j\omega\mu_o \vec{H} \\
 &= \frac{\partial E_\rho}{\partial z} - \frac{\partial E_z}{\partial \rho} = \frac{j\omega\mu_o}{2\pi\rho} I(z)
 \end{aligned}$$

$$\frac{\partial}{\partial \rho} E_z(\rho, z) = \frac{1}{j\omega\epsilon_0} \frac{d^2 I(z)}{dz^2} \frac{1}{2\pi\rho} - \frac{j\omega\mu_o}{2\pi\rho} I(z)$$

which yields:

$$E_z(\rho, z) = \frac{1}{2\pi} \left[\frac{1}{j\omega\epsilon_0} \frac{d^2}{dz^2} I(z) - j\omega\mu_o I(z) \right] \ln\left(\frac{\rho}{a}\right) \quad (\text{A5})$$

by enforcing the boundary condition $E_z(a, z) = 0$.

REFERENCES

- [1] D. C. Chang, "On the electrically, cylindrical antenna," *Radio Sci.*, vol. 2, no. 9, pp. 1043–1060, Sep. 1967.
- [2] D. C. Chang, "On the electrically thick monopole: Part I—Theoretical Study," *IEEE Trans. Antennas Propag.*, vol. 16, no. 1, pp. 58–64, Jan. 1968.
- [3] D. C. Chang, "On the electrically thick monopole: Part II—Experimental study," *IEEE Trans. Antennas Propag.*, vol. 16, no. 1, pp. 64–71, Jan. 1968.
- [4] D. H. Werner, "An exact formulation for the vector potential of a cylindrical antenna with uniformly distributed current and arbitrary radius," *IEEE Trans. Antennas Propag.*, vol. 41, no. 8, pp. 1009–1018, Aug. 1993.
- [5] E. C. Jordan and K. C. Balmain, *Electromagnetic Waves and Radiating Systems*. Englewood Cliffs, NJ, USA: Prentice-Hall, Inc. 1968, pp. 333–337.
- [6] R. W. P. King and C. W. Harrison, *Antennas and Waves: A Modern Approach*. Cambridge, MA, USA: MIT Press, 1969.
- [7] Q. Balzano, O. Garay, and K. Siwiak, "The near field of dipole antennas. Part I: Theory," *IEEE Trans. Veh. Technol.*, vol. VT-30, no. 4, pp. 161–182, Nov. 1981.
- [8] Q. Balzano, O. Garay, and K. Siwiak, "The near field of omnidirectional helical antennas," *IEEE Trans. Veh. Technol.*, vol. VT-31, no. 4, pp. 173–184, Nov. 1982.
- [9] A. Schwab, C. Fuchs, and P. Kistenmacher, "Semantics of the irrotational component of the magnetic vector potential," *IEEE Antennas Propag. Mag.*, vol. 39, no. 1, pp. 46–51, Feb. 1997.
- [10] L. B. Felsen and N. Marcuvitz, *Radiation and Scattering of Waves*. Englewood Cliffs, NJ, USA: Prentice Hall, 1973, ch. 1, p. 89.
- [11] A. G. Williamson, "On the aperture field of solid cylindrical antenna," *IEEE Trans. Antennas Propag.*, vol. 23, no. 6, pp. 862–864, Nov. 1975.
- [12] R. F. Harrington, *Time Harmonic Electromagnetic Fields*. New York, NY, USA: McGraw-Hill, 1961, ch. 5, section 5-11, p. 244.
- [13] R. F. Harrington, *Time Harmonic Electromagnetic Fields*. New York, NY, USA: McGraw-Hill, 1961, ch. 2, section 2-9, p. 77.
- [14] N. W. McLachlan, *Bessel Functions for Engineers*, 2nd ed. Oxford, U.K.: Oxford Univ. Press, 1961, section I.2, p. 5.
- [15] N. W. McLachlan, *Bessel Functions for Engineers*, 2nd ed. Oxford, U.K.: Oxford Univ. Press, 1961, section II.1 pp. 25–26.



ALESSANDRA PAFFI received the Laurea degree (*cum laude*) and the Doctoral degree in electronic engineering from the Sapienza University of Rome, Italy, in 1999 and 2005, respectively.

From 2005 to 2010, she was a Postdoctoral Fellow with the Italian Inter-University Center of Electromagnetic Fields and Biosystems (ICEmB), University of Genoa, and the Department of Electronic Engineering, Sapienza University of Rome, where she was an Assistant Professor with the Department of Information Engineering,

Electronics and Telecommunications (DIET) from 2011 to 2014. From 2019 to 2022, she was a Postdoctoral Fellow with ICEmB, University of Genoa. She is currently an Assistant Professor with DIET, Sapienza University of Rome, where she teaches “Electromagnetic Compatibility for Biomedical Apparatuses” for the Biomedical Engineering Course. Her main research interests include theoretical and experimental studies for modeling interactions between EM fields and biological systems. Her special interest is devoted to the design and fabrication of EM field exposure systems in the radiofrequency range.



EDUARDO CARRASCO (Senior Member, IEEE) received the bachelor's degree in telecommunication engineering from the National Autonomous University of Mexico, Mexico City, in 2000, and the Ph.D. degree in telecommunication engineering from the Universidad Politécnica de Madrid (UPM), Madrid, Spain, in 2008. From January to April 2008, he visited the Microwave Engineering Laboratory, University of Perugia, Italy. From June 2009 to June 2012, he was employed with the Electromagnetism and Circuits

Theory Department, UPM, as a Postdoctoral Researcher. From 2012 to 2014, he was with the Swiss Federal Institute of Technology Lausanne, Switzerland, as a Marie-Curie Fellow. He was with the Foundation for Research on Information Technologies in Society, Zürich, Switzerland, from January 2015 to September 2017, as an Electromagnetic, Dosimetry, and Antenna Researcher. Since October 2017, he has been with the Information Processing and Telecommunications Center, UPM, where he is currently an Associate Professor. He has participated in various projects supported by the Spanish Government, the Mexican Council of Science and Technology, the European Union's Sixth, Seventh, and H2020 Framework Programs, the European Space Agency and industry (Metawave, Huawei, and Schmid & Partner). His main research interests include the design of reconfigurable antenna arrays, including reflect- and transmit-arrays, from microwave to terahertz frequencies, as well as EMF exposure, hyperthermia treatment planning, and other bioelectromagnetics topics.



QUIRINO BALZANO (Life Fellow, IEEE) was born in Rome, Italy, in December 1940. In 1965, he received the Laurea of Doctoral in electronics engineering from the University of Rome, La Sapienza, Rome, Italy.

During 1966, he was with FIAT, SpA, Turin, Italy. From 1967 to 1974, he was with the Missile Systems Division, Raytheon Corporation, Bedford, MA, USA. He was involved in the research and development of planar and conformal phased arrays for the Patriot and other weapon systems.

In 1974, he joined Motorola, Inc., Plantation, FL, USA. In 1987, he became a Vice President of the technical staff and in 1993 Corporate Vice President and a Director of the Florida Research Laboratories. He retired from Motorola in February 2001. Since August 2002, he has been with the Electrical and Computer Engineering Department, University of Maryland at College Park, Maryland, USA, where he is a Senior Staff Researcher and teaches a graduate course on antennas. He has written more than 50 papers on RF dosimetry near electromagnetic sources and the biological effects of RF energy. His main interests are in the biological effects of human exposure to RF electromagnetic energy and the safe use of wireless technology.

Dr. Balzano received the IEEE Vehicular Technology Society Paper Prize Award in 1978 and 1982 and a certificate of merit from the Radiological Society of North America in 1981 for the treatment of tumors with RF energy. In 1995, he received the Best Paper of the Year Award from the IEEE EMC Society. He has 31 patents in antenna and IC technology and has authored or coauthored more than 100 publications.

Open Access funding provided by ‘Consiglio Nazionale delle Ricerche-CARI-CARE’ within the CRUI CARE Agreement